

BMTree: Designing, Learning, and Updating Piecewise Space-Filling Curves for Multi-Dimensional Data Indexing

Jiangneng Li, Yang Liu, Zheng Wang, Gao Cong, Cheng Long, Walid G. Aref, *Fellow, IEEE*, Han Mao Kiah, and Bin Cui, *Fellow, IEEE*

Abstract—Space-filling curves (SFC, for short) have been widely applied to index multi-dimensional data, which first maps the data to one dimension, and then a one-dimensional indexing method, e.g., the B-tree indexes the mapped data. Existing SFCs adopt a single mapping scheme for the whole data space. However, a single mapping scheme often does not perform well on all the data space. In this paper, we propose a new type of SFC called piecewise SFCs that adopts different mapping schemes for different data subspaces. Specifically, we propose a data structure termed the Bit Merging tree (BMTree) that can generate data subspaces and their SFCs simultaneously, and achieve desirable properties of the SFC for the whole data space. Furthermore, we develop a reinforcement learning-based solution to build the BMTree, aiming to achieve excellent query performance. To update the BMTree efficiently when the distributions of data and/or queries change, we develop a new mechanism that achieves fast detection of distribution shifts in data and queries, and enables *partial* retraining of the BMTree. The retraining mechanism achieves performance enhancement efficiently since it avoids retraining the BMTree from scratch. Extensive experiments show the effectiveness and efficiency of the BMTree with the proposed learning-based methods.

Index Terms—Learned Index, Space-Filling Curves.

I. INTRODUCTION

A Space-filling curve (SFC, for short) is a way to map a multi-dimensional data point \mathbf{x} to a one-dimensional value, say v that can be represented by a mapping function $T : \mathbf{x} \mapsto v$. SFC mappings been widely used for multi-dimensional indexing. The idea is to first map multi-dimensional data points to one-dimensional values using the SFC mapping function, and then use one-dimensional indexing methods, e.g., a conventional B-Tree [1] or any of the recent learned indexes [2, 3, 4, 5], to index the mapped values. This has been explored both in the literature [6, 7, 8, 9, 10, 11, 12] and by various database systems, e.g., PostgreSQL [13], Amazon DynamoDB [14], Apache HBase [15], and many other systems.

There are extensive studies on designing SFCs, e.g., the Z-curve [16, 17, 18], the C-curve [19], and the Hilbert curve [19, 20, 21, 22]. For example, the Z-curve adopts a *bit interleaving* mapping scheme [23] that first converts the

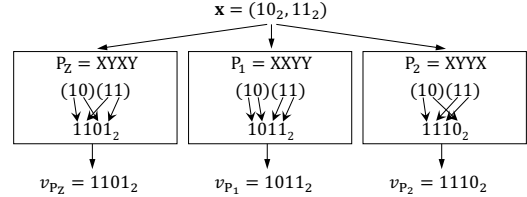


Fig. 1: The example illustrates mapping a point using various Bit Merging Patterns (BMP), where each mapping corresponds to a difference SFC. The illustrated BMP mappings are as follows: P_Z (XYXY) is the BMP of the Z-curve, XXYY is the BMP of the saw-tooth curve (a column-wise scan [19]), and XYYX is the third BMP.

dimensions of input data to *bit strings*. Refer to Figure 1 for illustration, where data point $\mathbf{x} = (2, 3)$ is converted into its two corresponding binary strings (one string per coordinate) with 2 bits for each dimension: $(10_2, 11_2)$. Then, the bit interleaving merges bits alternatively from the different bit strings to form one SFC value (in Figure 1, the bit interleaving adopts the XYXY merging scheme that merges the bit strings XX and YY to the SFC value XYXY, e.g., mapping Point \mathbf{x} to 1101_2).

However, one common problem is that each SFC has its own fixed mapping scheme/function that cannot be adjusted to fit different datasets. The choice of one SFC for a dataset significantly affects query performance, and no single SFC can dominate the performance for all datasets and all query workloads (as shown in Fig. 2). To tailor a new SFC to fit the data and query workload properties, QUILTS [24] extends bit interleaving by considering other ways of merging bit strings. For example, instead of merging bits following XYXY, we can merge bits by following XXYY or XYYX to generate different SFC values at different regions of the multi-dimensional data set. Each pattern of merging bits is termed a *bit merging pattern* (BMP, for short), where each BMP can describe a different SFC (as will be explained in Section II in greater detailed). QUILTS evaluates all the candidate SFCs described by BMPs based on a given workload and data, and selects the optimal one using heuristic methods.

QUILTS proposes to use multiple SFCs at the same time to index one data set so that the resulting mixed SFC is query-aware and is skew-tolerant for a given query pattern. However, the resulting SFC is static and hence does not change if the data distribution or the query workload changes over time.

J. Li, Y. Liu, Z. Wang, G. Cong, C. Long, and H.M. Kiah are with Nanyang Technological University, Singapore, 639798. E-mail: {jiangnen002@e., s230084@e., zheng011@e., gaocong@, c.long@, HMKiah@}ntu.edu.sg; W. G. Aref is with Purdue University, West Lafayette, IN, USA, 47907. E-mail: aref@purdue.edu; B. Cui is with School of Computer Science, Peking University, Beijing, China, 100871. E-mail: bin.cui@pku.edu.cn.

QUILTS makes the first attempt to utilize data and query workload properties to select an optimal SFC. However, like other SFCs, QUILTS applies a single BMP for the entire data space (i.e., QUILTS applies one BMP to compute the SFC values of all data points). Optimal SFCs may differ for different data subspaces. A detailed example of this situation is given in Section III-A that illustrates this problem. Another issue of QUILTS is that it does not provide an effective way of generating and evaluating candidate SFCs. The heuristic rules used by QUILTS are designed for very specific types of window queries (e.g., with a fixed area) and do not fit general query processing scenarios, where the workload includes more than one query type (with different areas or aspect ratios). For example, a heuristic rule used by QUILTS assumes that grid cells intersecting with a query should be continuous in SFC order, which may not hold for queries with different aspect ratios (this is elaborated on in greater detail in Section III-A). Further, QUILTS does not consider the scenario where the distributions of data and/or queries are changed, which results in sub-optimal query performance if the SFC is not updated.

To address the limitations of an SFC with a single BMP, i.e., a single mapping scheme, our idea is to design different BMPs for different subspaces based on the data and query workload features, aiming to optimize query performance. The resulting SFCs used in the BMTree would comprise multiple BMPs, each corresponding to a subspace that we refer to by a *piecewise* SFC. We focus on three aspects of the piecewise SFC construction framework: (1) Designing the piecewise SFC: We propose a binary tree structure to help construct and design a piecewise SFC. (2) Learning the piecewise SFC. We design a data-driven learning-based method that can automatically construct the piecewise SFC according to the query workload to optimize query performance. (3) Updating piecewise SFC: We develop a mechanism aiming to efficiently update the piecewise SFC w.r.t. the updated query and data scenario.

A. Designing Piecewise SFCs

How to design effective BMPs for different subspaces, while guaranteeing desirable properties of the overall mapping function to indexing data, is non-trivial. To achieve that, we propose to seamlessly integrate subspace partitioning and BMP generation. We develop a new structure termed the *Bit Merging Tree* (BMTree, for short) to recursively generate both the subspaces and the corresponding BMPs. In the BMTree, (1) Each node represents a bit from the binary string of the selected dimension, and its bit value (0 or 1) partitions the data at the node into two child nodes, and (2) Each leaf node represents a subspace, and the sequence of bit string from the root to the leaf node represents the BMP for the subspace.

Further, we prove that the Piecewise SFC modeled by the BMTree maintains two desirable properties: Monotonicity [25] and Injection. Monotonicity is a desirable property for designing window query algorithms, which guarantees that the SFC values of data points in a query rectangle fall in the SFC value range formed by two boundary points of the query rectangle. Combining different SFCs from different subspaces to obtain a

final SFC for the whole space may lead to the risk of breaking the monotonicity property. Similarly, it may also lead to an injection violation, i.e., that the mapping function may not return a unique mapped value for each input. We construct the BMTree in a principled way such that the two properties are guaranteed.

B. Learning Piecewise SFCs

To address the limitation of heuristic algorithms in the SFC design, we propose to model building the BMTree as a Markov decision process (MDP, for short) [26], aiming to develop data-driven solutions for designing suitable BMPs for different subspaces. Specifically, we define the states, the actions, and the rewards signals of the MDP framework to build the BMTree such that the generated BMTree can optimize query performance. We leverage reinforcement learning and Monte Carlo Tree Search (MCTS, for short) [27], to learn a performance-aware policy and avoid local optimal settings. To improve performance, we design a greedy action selection algorithm for MCTS. Moreover, to improve training efficiency, we define a metric termed *ScanRange* as a proxy of the query performance (e.g., I/O cost or query latency), and apply ScanRange for the computation of rewards.

C. Updating Piecewise SFCs

In situations where the distributions of data and queries change [28], the previously learned module faces an issue of having sub-optimal performance. Fully retraining a BMTree poses efficiency challenges due to the BMTree training cost, and the need to update all SFC values of data points maintained in the index. To address this issue, we propose a novel mechanism aligned with the BMTree structure that enables partial retraining, and hence reducing the overall cost. First, we introduce a distribution shift score to quantify the shift degree, and decide if retraining is necessary. Then, we develop an optimization potential score to identify which nodes of BMTree, when optimized, can significantly enhance query performance. We partially delete the nodes of the BMTree that need to be retrained, and develop an adapted training reinforcement learning environment (with the states, actions, and rewards adapted for partial retraining) and regenerate the BMTree with respect to the updated data and query workloads.

The main contributions of this paper are as follows:

- (1) We propose the idea of piecewise SFCs that allows to design different BMPs for different subspaces by considering the data and query workload properties to deal with non-uniformly distributed data and query workloads.
- (2) To design piecewise SFCs, we introduce the BMTree to partition the data space into subspaces, and generate a BMP for each subspace. We prove that the piecewise SFC represented by a BMTree satisfies two properties, namely injection and monotonicity.
- (3) To build a BMTree, we develop an RL-based solution by modeling BMP design as a MDP, and design an MCTS-based BMTree construction algorithm. We develop the ScanRange metric to efficiently measure the window query performance

on an SFC. As a result, the ScanRange metric speeds up the learning procedure.

(4) To efficiently update a BMTree, we develop a mechanism that allows partially retraining of the BMTree when data and/or query distributions shift, and enhances the query performance with reasonable retraining costs.

(5) We integrate our learned SFCs into the B⁺-Tree index inside PostgreSQL and inside the learned spatial index RSMI [12]. Experimental results under both settings consistently show that the BMTree outperforms the baselines in terms of query performance. Further, the partial retraining mechanism achieves notable performance enhancement that is competitive to full retraining while achieving over 2× speedup compared to full retraining.

Compared to the previously published paper [29], this paper introduces over 35% new content. We extend the BMTree by incorporating a novel reconstruction mechanism that enables it to quickly adapt itself to distribution shifts and achieves better query performance, which is not supported by other SFC methods. We also include additional experiments to evaluate the proposed mechanism under different shift settings, including data shift, query shift, and their combination.

II. PROBLEM STATEMENT & PRELIMINARIES

A. Problem Definition

Let \mathcal{D} be a database, where each data point $\mathbf{x} \in \mathcal{D}$ has n dimensions, denoted by $\mathbf{x} = (d_1, d_2, \dots, d_n)$. For ease of presentation, we consider only 2-dimensional data points $\mathbf{x} = (x, y)$, that can be easily extended to n dimensions. \mathbf{x} can be converted to bit strings as: $\mathbf{x} = ((x_1x_2 \dots x_m)_2, (y_1y_2 \dots y_m)_2)$, where each x_i, y_j ($1 \leq i, j \leq m$) are 0 or 1 (i.e., $x_i, y_j \in \{0, 1\}$) and m is the length of the bit string that is dependent on the cardinality of the dimensions x and y . Take $\mathbf{x} = (4, 5)$ for example, it can be converted in base 2 to $\mathbf{x} = (100_2, 101_2)$. In previous studies on SFC based multidimensional indexes, e.g., [1, 23, 30], values of data points are typically mapped to fine-grained grid cells for discretization. SFC maps \mathbf{x} into a scalar value v (called SFC value) with a mapping function $C(\mathbf{x}) \rightarrow v$. An SFC value v can be used as the key value of data \mathbf{x} to determine the order of \mathbf{x} in \mathcal{D} .

Problem 1 (SFC Design): Given a database \mathcal{D} and a query workload Q , we aim to develop a mapping function T that maps each data point $\mathbf{x} \in \mathcal{D}$ into an SFC value v , such that with an index structure (e.g., a B⁺-Tree) built on the SFC values of that data points in \mathcal{D} , the query performance (e.g., I/O cost and querying time) on Q is optimized.

B. Preliminaries on SFC

We present two desired properties for a mapping function T , namely *Injection* and *Monotonicity*. Then, we describe the curve design methods in the Z-curve and Quilts that also satisfy these properties.

Injection¹. An SFC design is expected to satisfy the injection property that guarantees a unique mapping from \mathbf{x} to v . This

is to ensure that each SFC value v can be used as a key value of \mathbf{x} for ordering and indexing data. It is defined as follows.

Definition 1 (Injection): Given a function $C : \mathbf{x} \rightarrow v$, C is injective if \mathbf{x} maps to a unique value v , s.t. $\forall \mathbf{x}_1 \neq \mathbf{x}_2, C(\mathbf{x}_1) \neq C(\mathbf{x}_2)$.

The injection property is desirable for an index to narrow the search space for better query performance. Consider an extreme situation where all data points map to the same value. Then, an index based on the SFC values cannot narrow the search space for a query.

Monotonicity. The monotonicity [25] is defined as follows.

Definition 2 (Monotonicity): Given two n -dimensional data points (denoted as \mathbf{x}' and \mathbf{x}''), whose SFC values are denoted by $C(\mathbf{x}')$ and $C(\mathbf{x}'')$. When a mapping function C holds monotonicity, if $d'_i \geq d''_i$ is satisfied for $\forall i \in [1, n]$, it always has $C(\mathbf{x}') \geq C(\mathbf{x}'')$.

Maintaining monotonicity is a desirable property for mapping data points to SFC values as explained below. Assuming the origin of the space is at the lower left, given a 2-dimensional window query represented by its minimum (bottom-left corner) and maximum (top-right corner) points (i.e., $\mathbf{q}_{min} = (x_{min}, y_{min})$, $\mathbf{q}_{max} = (x_{max}, y_{max})$). Let $\mathcal{P} = \{(x, y) \mid x_{min} \leq x \leq x_{max}, y_{min} \leq y \leq y_{max}\}$ denotes the query results bounded by the query window. If the monotonicity property holds, the result points in \mathcal{P} are within the range bounded by the SFC values of \mathbf{q}_{min} and \mathbf{q}_{max} . The reason is that for any data point $\mathbf{p} \in \mathcal{P}$, whose SFC value $C(\mathbf{p})$ always holds that $C(\mathbf{q}_{min}) \leq C(\mathbf{p}) \leq C(\mathbf{q}_{max})$. The property is desirable since it enables us to design simple and efficient algorithms for processing a window query by checking data points whose SFC values are within the bounded range only; Otherwise, the algorithm does not work. For example, the Hilbert curve and its variants [19, 20, 21] do not satisfy the monotonicity property, which makes it hard to identify the scanning range for a window query in the space of their SFC values, and requires maintaining additional structure to design more complicated algorithms [32].

Computing SFC values in the Z-curve [16, 17, 18] and in QUILTS [24]. Both Z-curve and QUILTS guarantee the injection and monotonicity properties. Figure 1 exemplifies how the Z-curve and QUILTS map a data point \mathbf{x} to a scalar SFC value v . The curve design in the Z-curve and QUILTS are presented as follows.

The SFC value of \mathbf{x} in the Z-curve is computed via bit interleaving, which generates a binary number consisting of bits (0 or 1) filled alternatively from each dimension's bit string. The Z-curve value of a 2-dimensional data point \mathbf{x} is computed by Function C_z :

$$C_z(\mathbf{x}) = (x_1y_1x_2y_2 \dots x_my_m)_2 \quad (1)$$

It assumes that all dimensions have the same bit-string length, and the zero-padding technique is usually applied to fit the length equally by padding zeros at the head of each bit string.

QUILTS generalizes the bit interleaving pattern of the Z-curve to more general *bit merging pattern*, each of which represents a way of merging bits. For example, for two-dimensional data, QUILTS defines a bit merging pattern as follows.

¹This property is defined on discretized input. No injection is guaranteed in continuous space since no bijection mapping exists between \mathbb{R} and \mathbb{R}^n [31].

Definition 3 (Bit Merging Pattern): A bit merging pattern (BMP) is a string P of length $2m$ over the alphabet $\{X, Y\}$ s.t. it contains exactly m X 's and m Y 's. Given a BMP point $P = p_1 p_2 \dots p_{2m}$, the SFC described by P is defined as follows. We set

$$C_P(\mathbf{x}) = (b_1 b_2 \dots b_{2m})_2 \quad (2)$$

according to the following rule: (1) Since P contains exactly m X 's, we let $I = \{i_1, \dots, i_m\}$ be the list of ordered indices such that $p_{i_\ell} = X$. Then, we set $b_{i_\ell} = x_\ell$ for $1 \leq \ell \leq m$. (2) Similarly, for the value of y , we consider $J = \{j_1, \dots, j_m\}$ where $p_{j_\ell} = Y$, and assign b_{j_ℓ} the bit value of y_ℓ . For example, given the BMP point $P = XXYX$, the value of data point \mathbf{x} computed by C_P is $C_P(\mathbf{x}) = (x_1 x_2 y_1 y_2)_2$. Notice that both x and y are subsequences of $T_P(\mathbf{x})$.

SFCs represented with different BMPs form an SFCs set. QUILTS considers this set and selects the optimal SFC evaluated on a given query workload as the output curve. We prove the monotonicity of SFCs with BMPs, which guarantees the monotonicity property of our method in Section VII. The detailed proof is given in [29].

Lemma 1 (Monotonicity of SFCs with BMPs): An SFC with a BMP achieves the monotonicity property.

III. MOTIVATION AND METHOD OVERVIEW

A. Motivations and Challenges

Motivation 1: Piecewise SFC Design. QUILTS and earlier SFCs based on BMPs only use one BMP to compute SFC values for all data points, which may not perform well for query processing.

Example 1: Figure 2 shows a 4×4 grid space, where the green and yellow dashed rectangles represent two window queries Q_1 (horizontal) and Q_2 (vertical), respectively. The red lines represent the ordering of grid cells w.r.t. three SFCs. For example, consider SFC-1, whose $P_1 = XYYX$ and the computed value for input $\mathbf{x} = ((x_1 x_2)_2, (y_1 y_2)_2)$ is $C_{P_1}(\mathbf{x}) = (x_1 y_1 y_2 x_2)_2$. Notice that in SFC-1, x_1 is put as the first bit in the combined bit string, and thus any data point with $x_1 = 0$ (that resides in the left half of Figure 2 (a)) will have a smaller mapped value than any data point with $x_1 = 1$ (that resides in the right side of Figure 2(a)). We label the grid ids based on the mapped values of grid cells computed by the SFC curves. As discussed in Section II-B, a typical algorithm first locates the grid ids on the minimum (bottom-left corner) and the maximum (top-right corner) points of a query window.

Different SFCs will result in accesses of different grid cells for answering the two window queries Q_1 and Q_2 . For instance, with SFC-1, Q_1 and Q_2 need 2 and 3 grid scans, respectively. With SFC-2 ($P_2 = XYYX$), Q_1 and Q_2 need 3 and 2 grid scans, respectively. Detailed computation can be found in [29]. Further, with SFC-1, cells in window of Q_1 are consecutive (cell 7 and 8 form a contiguous sequence, noted as 1 run in [19]), while cell 13 and 15 in Q_2 are not consecutive (2 runs). Query with 1 run means a contiguous memory access is available, which is preferred.

In the example, SFC-1 performs better for Q_1 while SFC-2 is better for Q_2 . A natural idea is whether we can combine the advantages from the two BMPs of SFC-1 and SFC-2, i.e.,

we use $XYYX$ to organize the data at the left hand side and $XYYX$ to organize the data at the right-hand side. The design will result in a *piecewise* SFC, shown as SFC-3 in Figure 2(c). With SFC-3, we need 2 grid scans for both Q_1 and Q_2 . This example motivates the need for designing a piecewise SFC.

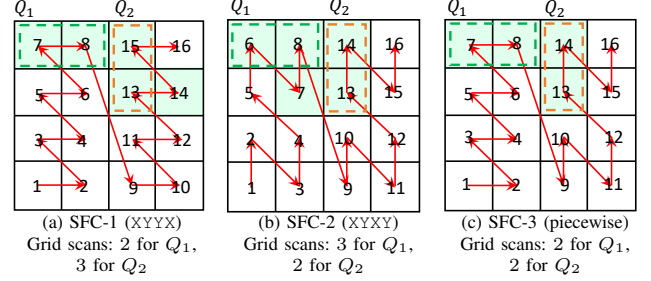


Fig. 2: Motivation for piecewise SFCs, SFC-1 is described by the BMP $XYYX$ while SFC-2 by $XYYX$. In contrast, SFC-3 (ours) is described by two BMPs: left by $XYYX$ and right by $XYYX$, where the green shade highlights the scanned grids.

Motivation 2: Learning-based Method for Piecewise SFC Construction. Classic SFCs (Z-curve, Hilbert curve, etc.) are based on a single scheme and fail to utilize the underlying database instance to design the SFC. In contrast, QUILTS proposes to utilize the given database and query workload to evaluate and select an SFC from an SFC set in which each SFC is described by a BMP. However, QUILTS does not directly evaluate SFC w.r.t. query performance but uses instead heuristic rules to generate candidate SFCs. The heuristic rules will select BMPs such that the resulting grid cells intersecting with a query would be continuous in the curve order, and hence results in fewer grid scans. These heuristics only work for query workloads containing limited types of window queries (e.g., with the same aspect ratio), and are not effective under general situations (where more than one query type with different aspect ratios and region areas exist). Due to these limitations, it calls for more principled solutions to utilize database and query workloads for generating and selecting an SFC. Learning-based methods would be promising for this purpose.

Motivation 3: Efficient Piecewise SFC Update. The distribution shift issue exists when maintaining data-driven learned indexes. When distribution shift happens, the performance of the learned modules can become suboptimal. A retraining procedure is preferred if the performance decreases to a certain degree. However, retraining the BMTree from scratch can be costly. Moreover, in cases where distribution shifts occur unevenly across subspaces (e.g., some subspaces with significant distribution shifts while others with mild shifts), not all BMPs require redesign. Two examples are given in Fig. 3 to illustrate the uneven shifts of data and query, respectively. In Fig. 3a, the data located in the left half of the space shifts from being uniformly distributed to being non-uniformly distributed. In Fig. 3b, the query located in the left half of the space has shifted not only the spatial distribution of the queries (considering the center point of each query rectangle) but also the categories of the queries (from Type 1 to Type 2

with different aspect ratios). These distribution shifts can lead to a decrease in performance of the SFC learned for the case of historical data and query distributions. The issue calls for a solution to provide an efficient way to update the BMTree w.r.t. distribution shifts. Additionally, it is preferable if the solution allows for the partial redesign of the BMTree while keeping a portion unchanged so that only the data points located in the retrained subspaces need to update their SFC values to maintain the corresponding indexes.

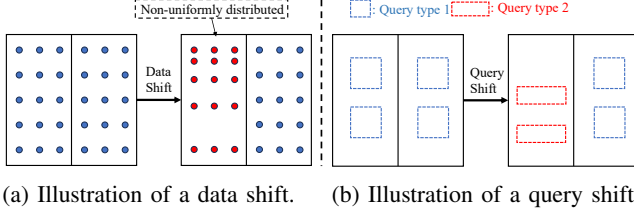


Fig. 3: Examples of distribution shifts of both data and query workloads over different subspaces.

Challenges. Piecewise SFC design gives rise to three challenges as discussed in the introduction section. (1) How to partition the space and design an effective BMP for each subspace? The piecewise SFC design needs to consider both space partitioning and BMP generation. (2) How to design piecewise SFCs such that the two desirable properties, namely, monotonicity and injection, still hold? (3) How to design a data-driven approach to automatically build the BMTree, given a database and query workloads? (4) How to identify the appropriate subspace for the partial retraining of the piecewise SFC without compromising its properties?

B. Overview of the Proposed BMTree

The Bit Merging Tree (BMTree) for Piecewise SFC Design.

To address the first challenge, we propose a novel way of seamlessly integrating subspace partitioning and BMP generation by constructing the BMTree; a binary tree that models a piecewise SFC. Each node of the BMTree is filled with a bit from a dimension. The filled bit partitions the space into two subspaces corresponding to two child nodes. The left branch is the subspace where data points have a bit value of 0 and the right branch with 1. The BMTree partitions the whole data space into subspaces, each corresponding to a leaf node with its BMP being the concatenated bit sequence from the root to the leaf node. We present the BMTree structure in Section IV. Furthermore, the BMTree mechanism guarantees that the generated piecewise SFC satisfies the two properties that address the second challenge. We prove that the piecewise SFC represented by a BMTree satisfies both monotonicity and injection in Section VII.

RL-based Algorithm for Constructing a BMTree. To address the third challenge, we design a learning-based method that learns from data and query workloads to build the BMTree. We model the building of the BMTree as a Markov Decision Process [26]. The process of building a BMTree comprises a sequence of actions to select bits for tree nodes by following a top-down order. To learn an effective policy

for building the BMTree, we propose a new approach for integrating a greedy policy into the Monte Carlo Tree Search (MCTS) framework [27]. Specifically, we develop a greedy policy that selects an action to fill a bit for each node during tree construction. For each node, the greedy policy chooses the bit that achieves the most significant reward among all the candidate bits. Afterwards, we apply the greedy policy as a guidance policy and use MCTS to optimize the BMTree with the objective of providing good query performance and avoiding local optima. Moreover, we introduce a fast computing metric, termed ScanRange, to speedup reward generation. We present the proposed solution in Section V and its time complexity analysis in Section VII.

Partially Retraining a BMTree for Piecewise SFC Update.

To address the last challenge, we develop a mechanism to efficiently update the BMTree. First, we propose a principal way that measures the shift of the subspace modeled by each BMTree node on query and data. A shift score measuring the distribution shift degree is introduced based on Jensen–Shannon (JS) divergence [33] that is a widely used tool for measuring the similarity between distributions. Then, the mechanism detects the nodes with largest performance optimization potentiality. Then, we partially delete the nodes of the BMTree that need to be retrained, and apply an adapted RL framework to regenerate the deleted BMTree parts with respect to the updated database scenario. The structure of the BMTree ensures that the regenerated piecewise SFC retrains all desired properties, since the regenerated BMTree naturally models a piecewise SFC properly. We present the details of the retraining mechanism in Section VI.

IV. DESIGNING PIECEWISE SFC: BIT MERGING TREE (BMTree)

We present how to develop a piecewise SFC, modeled by the Bit Merging Tree (BMTree) that is a binary tree.

Designing a BMP. To design a BMP P , we need to decide which character (X or Y in the two-dimensional case) is filled in each position of P . A left-to-right design procedure decides the filling characters in the order from p_1 to p_{2m} . The key to BMP design is to have a policy deciding which dimension (X or Y) to fill into each position of P .

Designing piecewise SFC with multiple BMPs. Next, we discuss piecewise SFC design. As discussed in Section III-A, one challenge in designing a piecewise SFC is: How to handle two subtasks that are intertwined together, namely subspace partitioning and BMP design within each subspace? It is also challenging to guarantee that the piecewise SFC comprising different BMPs for different subspaces still satisfies both the injection and monotonicity properties. To address these challenges, we introduce a new solution to simultaneously generate the subspaces and design the BMPs for these subspaces.

We follow a left-to-right BMP design approach, and start with an empty string P . For example, if we fill X in the first position of P , Bit x_1 will be filled to the b_1 th position of P ; Then, the whole data space is partitioned into two subspaces w.r.t. the value of Bit x_1 , where one subspace corresponds to $x_1 = 0$ and the other corresponds to $x_1 = 1$. This partitioning

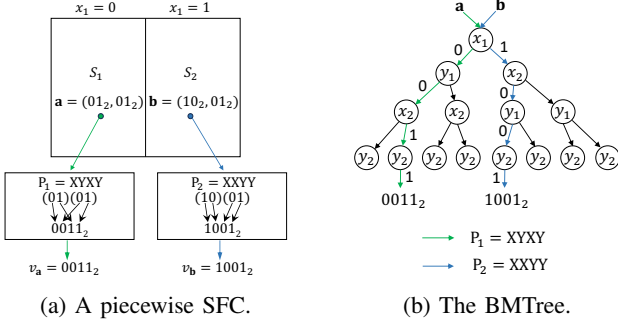


Fig. 4: (a) An example of a piecewise SFC that comprises two BMPs P_1 and P_2 for computing values of Data Points a and b . (b) A BMTTree that combines the two BMPs.

enables us to separately design different BMPs for the two subspaces. Notice that the BMPs for each subspace will share x as the first character, but can have distinct filling choices for the next $2m - 1$ characters. By recursively repeating this operation, we fill in the subsequent characters for each BMP for each subspace, thus generating multiple subspaces each with a different BMP. One advantage of this approach is that it seamlessly integrates subspace partitioning with BMP generation.

Example 2: Figure 4a gives an example of a piecewise SFC, where Dimensions x and y are bit strings of Length 2. First, x is selected, and then the whole space is partitioned w.r.t. value of Bit x_1 into two subspaces where Subspace S_1 corresponds to $x_1 = 0$ and Subspace S_2 corresponds to $x_1 = 1$. Next, we separately design BMPs for S_1 and S_2 , where all BMPs under S_1 share the first bit $x_1 = 0$ and BMPs under S_2 share the first bit $x_1 = 1$. We generate two example BMPs: $P_1 = XYXY$ for S_1 and $P_2 = XXYY$ for S_2 . Finally, we get a piecewise SFC that comprises C_{P_1} for S_1 and C_{P_2} for S_2 . This piecewise SFC represents the function: $C(\mathbf{x}) = \begin{cases} (x_1 y_1 x_2 y_2)_2 & \text{if } x_1 = 0 \\ (x_1 x_2 y_1 y_2)_2 & \text{if } x_1 = 1 \end{cases}$. Therefore, if Data Point a is located in S_1 , we apply C_{P_1} to compute a 's SFC value. Similarly, if Data Point b is in S_2 , we apply C_{P_2} to compute b 's SFC value.

To facilitate the process of designing piecewise SFCs, we propose the Bit Merging Tree (BMTTree) structure that is used to simultaneously partition the space and to generate the BMPs. Figure 4b gives the corresponding BMTTree for the example piecewise SFC of Figure 4a. Since the example piecewise SFC is developed with only 2 BMPs, the left subtree of the root node shares P_1 while the right subtree shares P_2 . Next, we present the BMTTree.

The Bit Merging Tree (BMTTree). The BMTTree is a binary tree that models a piecewise SFC C_T , and is denoted by T . The depth of a BMTTree T equals the length of a BMP, and is denoted by $2m$ for the 2-dimensional space. Every node of T corresponds to a bit of x_i or y_i , $1 \leq i \leq m$. The left (resp. right) child denotes the subspace with bit value 0 (resp. 1). Each path from the root node to a leaf node represents a BMP for the subspace of the leaf node, which is the concatenation of all the bits of the nodes in the path from root to leaf. The SFC value $C_T(\mathbf{x})$ of a data point \mathbf{x} is computed by traversing

a path of T as follows. We start from the root node, and for each traversed node, denoted by x_i , if $x_i = 0$, we visit the left child node; otherwise we visit the right child. When we reach a leaf node, the corresponding BMP of the traversed path is used to compute $C_T(\mathbf{x})$. The green path in Figure 4b is the path traversed for Point a that represents BMP P_1 while the blue path traversed for b represents P_2 .

To construct a BMTTree, we develop a breadth-first construction algorithm to assign bits to the BMTTree's nodes. Details (pseudo-code and the corresponding illustration) can be found in [29].

V. LEARNING PIECEWISE SFC: MCTS-BASED BMTREE CONSTRUCTION

It is difficult to design heuristic methods to construct the BMTTree to optimize the querying performance for a workload on a database instance. This could be observed from QUILTS that uses heuristic rules for a workload containing specific types of window queries only, and fails to directly optimize query performance. In contrast, we propose a reinforcement learning (RL) based method for learning a decision policy that builds the BMTTree to optimize query performance directly.

To allow an RL policy to construct the BMTTree, we model the BMTTree construction as a Markov decision process (MDP, for short). Then, we design a BMTTree construction framework with a model-based RL method, termed Monte Carlo Tree Search (MCTS, for short). Unlike traditional algorithms, e.g., greedy or A*, MCTS is an RL approach that demonstrates superior exploration-exploitation balance, mitigating the issue of local optimum. MCTS is well-suited for the problem at hand, and offers stable performance without extensive parameter tuning, compared with other RL algorithms, e.g., PPO [34].

Figure 5 gives the workflow of the MCTS-based BMTTree construction framework. We define one action that RL takes to be a series of bits that fill a level of nodes in the BMTTree, and the nodes of the next level are then generated. The action space size grows exponentially with the number of nodes. It becomes difficult for RL to learn a good policy with an enormously large action space. To address this issue, we design a greedy action selection algorithm that helps guide MCTS to search for good actions. Moreover, we design a metric, termed *ScanRange* to speed up reward computing.

BMTTree Construction as a Decision Making Process. We proceed to illustrate how we model BMTTree construction as a MDP, including the design of the *states*, *actions*, *transitions* and *reward*.

- **States.** Each partially constructed BMTTree structure T is represented by a state to map each tree with its corresponding query performance. The state of a BMTTree is represented by the bits filled to the BMTTree's nodes. For example, in Figure 5, the current (partially constructed) BMTTree's state is represented as $T = \{(1 : \underline{x}), (2 : \underline{xy})\}$, where \underline{x} and \underline{xy} are bits filled to the nodes in Levels 1 and 2.

- **Actions.** Consider a partially constructed BMTTree T that currently has N nodes to be filled. We define the actions as filling bits to these nodes. We aim to learn a policy that decides which bit to be filled for each node. Furthermore, the

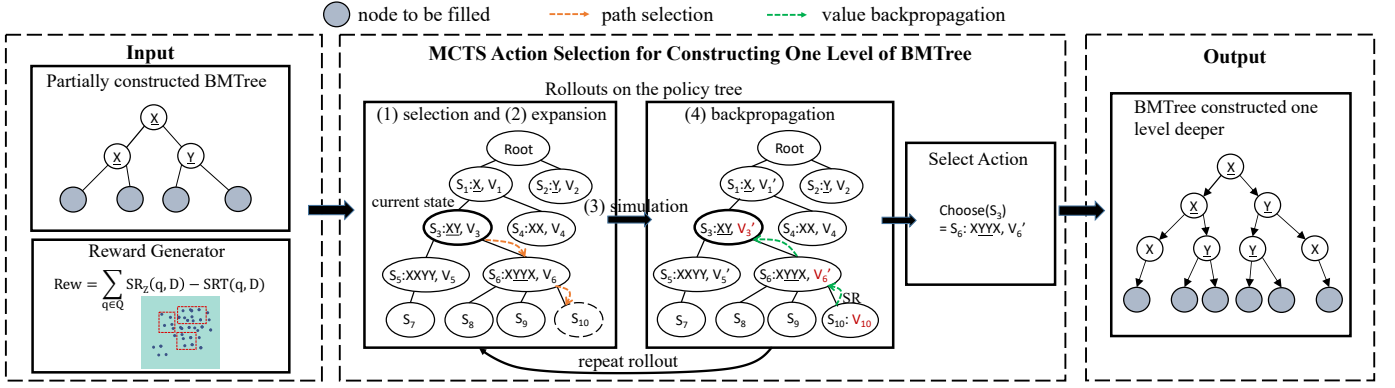


Fig. 5: Workflow of Monte Carlo Tree Search-Based BMTree construction.

policy decides if the BMTree will split the subspace of one tree node. If the policy decides to split, the tree node will generate two child nodes based on the filled bit \underline{b} , and the action is denoted by \underline{b} (with an underline). Otherwise, the tree node only generates one child node that corresponds to the same subspace as its parent, the action is denoted by b . During the construction, the policy will assign bits to all N nodes. The action is represented by $A = \{a_1, \dots, a_N\}$, $a_i = (\underline{b}_i, sp_i)$, where \underline{b}_i denotes the bit for filling Node n_i , and sp_i denotes whether to split the subspace. Given T with N nodes to be filled, the action space size is $(2n)^N$ where n is the dimension number, and a factor of 2 comes from the decision of whether or not to split the subspace.

- **Transition.** With the selected action A for the unfilled nodes in T , the framework will construct T' based on A . The transition is from the current partially constructed BMTree T to the newly constructed tree T' , denoted by $T' \leftarrow \text{Transition}(T, A)$. In our framework, we start from an empty tree, and construct the BMTree level at a time during the decision process. In each iteration, the action generated by the policy will fill one level of BMTree nodes (starting from Level 1), and will generate nodes one level deeper.

- **Rewards Design.** After T evolves into T' , we design the reward that reflects the expected query performance of T' to evaluate the goodness of Action A . One might consider executing queries using the corresponding BMTree to see how well the SFC helps decrease I/O cost. However, this is time-consuming. Thus, we propose a metric, that we term *ScanRange* (SR) that reflects the performance of executing a window query, and can be computed efficiently. We construct the reward based on T' 's SR . We define the function $SR_T(q, \mathcal{D})$ as taking a query q and a dataset \mathcal{D} as input, and outputs the *ScanRange* of q over \mathcal{D} .

Efficient Reward Computing. SR is computed as follows. Given a BMTree T , we randomly sample data points from \mathcal{D} with a sampling rate r_s . Then, the sampled data points are sorted according to their SFC values. To compute the SFC values on a partially constructed BMTree, we apply a policy extended from the Z-curve to the unfilled portions of the BMP in each subspace. Sorted data points are then evenly partitioned into $\frac{r_s |\mathcal{D}|}{|B|}$ blocks, where $|B|$ denotes the number of points per block. For a given Window Query q represented

by its minimum point \mathbf{q}_{min} and maximum point \mathbf{q}_{max} , we calculate the SFC value of the minimum (resp. maximum) point as $v_{min} = C_T(\mathbf{q}_{min})$ (resp. $v_{max} = C_T(\mathbf{q}_{max})$). We denote the blocks that v_{min} and v_{max} fall into by ID_{min} and ID_{max} , respectively. We calculate q 's SR given T and \mathcal{D} as $SR_T(q, \mathcal{D}) = ID_{max} - ID_{min}$. The calculation of SR is way cheaper than actually evaluating Query q .

We develop a reward generator based on the evaluated SR . We take the performance of the Z-curve as a baseline. Given the dataset \mathcal{D} and a query workload \mathcal{Q} . The generator sorts the data points based on their SFC values, and computes the reward as:

$$Rew = \sum_{q \in \mathcal{Q}} (SR_Z(q, \mathcal{D}) - SR_T(q, \mathcal{D})) \quad (3)$$

Intuitively, the reward is positive if the BMTree constructed by the policy achieves a lower SR than the Z-curve. This design allows the agent to assess the actual performance of the constructed BMTree compared to Z-curve. Empirical studies show that this choice helps the agent efficiently identify good actions. We normalize the reward by dividing the reward of the Z-curve.

Example 3: Refer to Figure 5. The partially constructed BMTree is represented by the bits filled to different levels, denoted by $T = \{(1 : \underline{X}), (2 : \underline{XY})\}$, where each tuple is the bits filled in the corresponding BMTree level. The learned policy selects the action $A = \underline{XYX}$. The next level of the BMTree is constructed based on A . The reward signal is computed based on the performance of the BMTree's newly added level. The BMTree will continue to be provided as input for constructing its next level.

We proceed to present the proposed MCTS framework, including a BMTree T under construction, a policy tree that helps to decide the action and gets updated gradually, and a reward generator that generates the reward based on T .

Policy Tree. MCTS [27, 35] is a model-based RL method. The high-level idea of MCTS is to search in a tree structure, where each node of the tree structure denotes a state. Given the current state, the objective of MCTS is to find the optimal child node (i.e., the next state) that potentially achieves an optimal reward. The structure that records and updates the historical states and their associated rewards is named *policy*

tree [35], where each child node denotes a next possible action (the design choice for the next level of the BMTree), and we define it as follows:

Definition 4 (Policy Tree): The policy tree is a tree structure that models the environment. Each node of the policy tree corresponds to a state, representing a current partially constructed BMTree. Moreover, every node stores: (1) Action A that constructs one more level of the BMTree, and (2) A reward value that reflects the goodness for choosing a node. The root node of the policy tree corresponds to an empty BMTree, and each path of the policy tree from the root node to the leaf node corresponds to a decision procedure of constructing a BMTree. The middle section of Fig. 5 illustrates an example of policy tree.

Rollouts. To choose an action, MCTS checks the reward that different action choices can achieve. To achieve this, MCTS will make several attempts in which it simulates several paths in the policy tree, and then checks if the attempted path results in better performance. Then, MCTS updates the policy tree based on the simulations, referred to as *rollout* in [27], indicating the operation that involves repeatedly selecting different actions and ultimately choosing the optimal one. A rollout consists of four phases: (1) *Selection* that selects the attempted path corresponding to a BMTree construction procedure, (2) *Expansion* that adds the unobserved state node to the policy tree, (3) *Simulation* that tests the selection's query performance, and (4) *Backpropagation* that updates the reward value. We proceed to present the design of each of these four steps.

(1) *Selection.* The selection step aims to select a path in the policy tree that potentially achieves good performance. Starting from the current state S_t with the initialized path: $\text{Path} = \{S_t\}$, we first check if all child nodes have been observed in the previous rollouts. If there are unobserved nodes, we choose one of them and add it to the path. Otherwise, we apply the Upper Confidence bounds applied to Trees (UCT) action selection algorithm [36] to select a child node that balances exploration vs. exploitation. Specifically, UCT selects the child node with the maximum value $v_{uct} = \frac{V_{t+1}}{\text{num}(S_{t+1})} + c \cdot \sqrt{\frac{\ln(\text{num}(S_t))}{\text{num}(S_{t+1})}}$. $S_{t+1} = \text{Transition}(S_t, A)$, where V_{t+1} is the reward value of the child node S_{t+1} evolving from S_t by Action A ; $\text{num}(S_{t+1})$ and $\text{num}(S_t)$ denote the times of observing Nodes S_{t+1} and S_t , respectively, during rollouts; c is a factor defaulted by 1. Then, the selected node S_{t+1} is added to the path: $\text{Path} = \{S_t \rightarrow S_{t+1}\}$. The selection step continues until the last node of Path is an unobserved node (the policy does not know the expected value of this node). Then, it returns the Path for the next step.

(2) *Expansion.* In the expansion step, the unobserved nodes in Path are added to the policy tree. The number of observations of each node S_t in Path, denoted as $\text{num}(S_t)$, is incremented by 1. Then, this value is used to compute the average reward.

(3) *Simulation.* We simulate the performance of the selected Path by constructing the BMTree based on the actions stored in the nodes of the path. Then, the constructed BMTree is input to the reward generator to compute the tree's SR metric.

(4) *Backpropagation.* In this step, we update the value of each

node in Path. We apply the maximum value update rule that updates the value of a state S_t with the maximum reward it gains from simulation, computed by $V'_t = \max(V_t, \text{Rew})$, where V_t is State S_t 's old value, Rew is the reward gained during the simulation, and V'_t is the updated value.

Example 4: Refer to Figure 5. State S_3 corresponds to the input partially constructed BMTree. During the rollouts, we select Path $\{S_3 \rightarrow S_6 \rightarrow S_{10}\}$ in the selection step. Then, it expands the new observed State S_8 to the policy tree in the expansion step. We construct the BMTree based on the selected path and compute SR. In the backpropagation step, the values of S_3 , S_6 and S_{10} are updated whose values are listed in red, based on the computed SR in S_{10} .

After the rollouts procedure, the algorithm selects the action with the highest reward, and then BMTree T is constructed accordingly. In the example, S_6 is selected with the largest value V'_6 compared to the other child nodes. Then, it returns Action XYX to build the BMTree one level deeper.

Greedy Action Selection. We design the greedy action selection algorithm (GAS, for short) for the selection step in rollouts for MCTS to find a good action for a partially constructed BMTree. Given T with N nodes to be filled, GAS generates an action A_g by greedily assigning a bit to each BMTree node that achieves the minimum SR compared to other bits when T is filled with that bit.

To summarize, the MCTS-based BMTree construction has two steps: BMTree initialization and MCTS-based BMTree learning. Its detailed pseudo-code can be found in [29].

VI. UPDATING PIECEWISE SFC

In this section, we proceed to handle BMTree maintenance. As described in Section III-A, with the change in distribution of the data and/or query workload, the performance of the BMTree is no longer optimal. Retraining the whole BMTree from scratch would be inefficient and would consume resources. To achieve efficient piecewise SFC update, we design a mechanism that partially retrains a BMTree based on the pre-trained BMTree instead of fully retraining a BMTree from scratch, while notably improving query performance under the new data and query distributions. We proceed to introduce: (1) Measurement of the degree of distribution shift that determines whether the BMTree nodes should be retrained; (2) Detection of which BMTree nodes to be retrained that identifies the nodes to be retrained for an optimal effectiveness-efficiency trade-off; and (3) Partial BMTree retraining that enables partial retraining of the selected BMTree nodes while maintaining the rest of the BMTree unchanged.

A. Assessment of the Distribution Shift

Partial retraining of a piecewise SFC requires retraining a portion of the piecewise SFC while maintaining the overall structure still a piecewise SFC. Furthermore, detecting the subspace that could improve query performance after being trained is non-trivial. To address these issues, we follow the pre-designed BMTree structure modeling, where we split the domain w.r.t. the structure of the BMTree. As in Section IV, different nodes of BMTree represent different subspaces. To

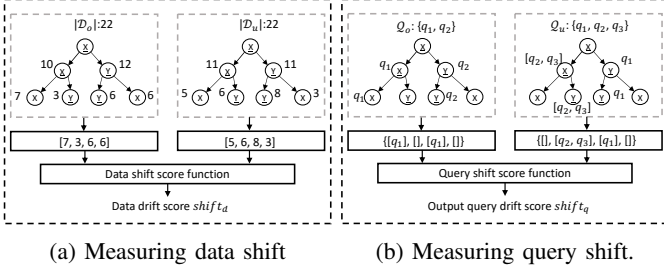


Fig. 6: Measuring distribution shifts within the BMTree.

achieve effective and efficient detection of the retraining subspace, we model the degree by which data and query distributions drift within the BMTree structure as follows.

Let N be a BMTree node that represents a subspace of the whole data space domain. Suppose an action is applied to N , and N is split into the two child nodes N_1 and N_2 , where each child node denotes half of the original subspace. With actions further assigned to N_1 and N_2 , the grandchild nodes of N split from N_1 and N_2 (4 grandchild nodes if N_1 and N_2 are all split) denote more fine-grained subspaces, respectively. We measure the distribution difference of the subspace denoted by N before and after the data or query is updated. We model the data and query distribution shifts of Node N as follows:

Modeling Data Shift. Suppose the split level is set to 2 that denotes that the data shift of a BMTree node N is computed w.r.t. the grandchild nodes 2 levels deeper than N (4 grandchild nodes by default). The historical and updated datasets are denoted as \mathcal{D}_o and \mathcal{D}_u , respectively. Refer to Fig. 6a. The data points are split w.r.t. the nodes. On the left side (resp. right side) of the figure, the \mathcal{D}_o (resp. \mathcal{D}_u) is split into four parts at Level 2 in the subtree, and we represent the distribution as $l_o^d = [\frac{7}{22}, \frac{3}{22}, \frac{6}{22}, \frac{6}{22}]$ (resp. $l_u^d = [\frac{5}{22}, \frac{6}{22}, \frac{8}{22}, \frac{3}{22}]$), where the distribution is normalized by the cardinality of the dataset. Note that the representation of the data will change if the action assigned to the sub-tree is different. Then, we apply the Jensen–Shannon (JS) divergence [33] to measure the data shift, defined as follows:

$$shift_d \triangleq D_{JS}(l_o^d || l_u^d) = \frac{1}{2} \left(D_{KL}(l_o^d || l_{mix}^d) + D_{KL}(l_u^d || l_{mix}^d) \right), \quad (4)$$

where D_{KL} denotes the Kullback–Leibler (KL) divergence function, defined as $D_{KL}(l_o^d || l_u^d) = \sum_i l_o^d[i] \cdot \log \frac{l_o^d[i]}{l_u^d[i]}$. l_{mix}^d denotes the mixed distribution of l_o^d and l_u^d : $l_{mix}^d = \frac{1}{2}(l_o^d + l_u^d)$. The larger the KL divergence $D_{JS}(l_o^d || l_u^d)$ is, the greater the difference between \mathcal{D}_o and \mathcal{D}_u .

Modeling Query Shift. For the query shift, we split the query set w.r.t. the BMTree nodes. Specifically, we compute the center point of each query, and divide the query set according to the center point, e.g., if the query is denoted by: $(x_{min}, y_{min}, x_{max}, y_{max})$, the center point is computed as: $(\frac{x_{min}+x_{max}}{2}, \frac{y_{min}+y_{max}}{2})$. Then, according to the grandchild nodes of N , the queries are split into 4 parts. Refer to Fig. 6b. On the left side of the figure, the old queryset $\mathcal{Q}_o = \{q_1, q_2\}$ is split into a list of four subsets $l_o^q = \{\{q_1\}, \{\}, \{q_2\}, \{\}\}$, while on right side the updated queryset $\mathcal{Q}_u = \{q_1, q_2, q_3\}$ is split as $l_u^q = \{\{\}, \{q_2, q_3\}, \{q_1\}, \{\}\}$. Unlike the measure

of data shift that directly compares the number of data points of each list element, we cluster the queries in each node into different clusters w.r.t. the area and the aspect ratio, and thus compute the JS divergence of each list element. Then, the JS divergence is averaged across the list elements:

$$shift_q \triangleq \frac{1}{|l_o^q|} \sum_i D_{JS}(l_o^q[i] || l_u^q[i]) \quad (5)$$

After modeling the distribution shifts of both data and queries, next we introduce how to decide the subspaces to be retrained. When the retraining procedure begins, the method will recursively compute the data and query shifts of nodes in the BMTree T under a Breadth-First Search (BFS) order. We restrict the distribution shift computation to a limited depth of nodes in T , since the nodes with larger depth represent small data subspaces, and will contribute limited improvement in performance. When both data and query are shifted, the shift scores of data and query are weight summed as the final shift score: $shift_m = \alpha \cdot shift_d + (1 - \alpha) \cdot shift_q$, where α is the weight parameter and is set by default to 0.5. Then, the nodes to be retrained are filtered based on this score. A shift threshold θ_s is set to filter the BMTree nodes. Nodes with shift score lower than θ_s are not retrained.

B. Deciding Which BMTree Nodes to Partially Retrain

Observe that the performance optimization potential of each node does not solely depend on the distribution shift degree. Instead, we propose to introduce a score based on the change in average ScanRange (SR_T) before and after the data and/or queries change, to measure fast the possible optimization potentials when retraining a node. The optimization potentials score OP on Node N is computed based on SR as follows:

$$OP(N, \mathcal{D}_o, \mathcal{D}_u, \mathcal{Q}'_o, \mathcal{Q}'_u, T) = \frac{\text{avg}_{q_u \in \mathcal{Q}'_u} SR_T(q_u, \mathcal{D}_u)}{\text{avg}_{q_o \in \mathcal{Q}'_o} SR_T(q_o, \mathcal{D}_o)}, \quad (6)$$

where \mathcal{Q}'_o (resp. \mathcal{Q}'_u) denotes the subset of historical (resp. updated) query workloads that the BMTree node N contains. $\text{avg}_{q_u \in \mathcal{Q}'_u} SR_T(q_u)$ and $\text{avg}_{q_o \in \mathcal{Q}'_o} SR_T(q_o)$ denote the average SR of \mathcal{Q}'_o and \mathcal{Q}'_u on BMTree T , respectively. Then, we compare the filtered BMTree nodes level at a time, and select the nodes with maximum OP score as the node to be retrained.

During retraining, to ensure a certain degree of efficiency improvement, a *retraining constraint ratio* R_{rc} is set to limit the retraining area of the retrained subspaces compared to a full retrain (e.g., if $r = 0.5$, the accumulated area of the retrained subspaces should not reach half the whole space).

The algorithm for detecting the BMTree nodes that need retraining is Listed in Algorithm 1. First, it initializes a queue \mathcal{N} with the root node of T (Line 1). Then, the algorithm processes level at a time of the BMTree (Lines 3 – 14). The leftmost node of \mathcal{N} is popped (Line 4), then the shift score s is computed by the ShiftScore function (with information about the dataset update and the BMTree given, as described before) (Line 5). Then, the nodes satisfying the threshold θ are added to \mathcal{L} , and the OP of N is computed w.r.t. Eq. 6 (Lines 6

Algorithm 1: Deciding on Which BMTree Nodes to Retrain.

input : n -dimensional old and updated dataset $\mathcal{D}_o, \mathcal{D}_u$, old and updated training workload $\mathcal{Q}_o, \mathcal{Q}_u$, BMTree T ;
output : Retrain nodes of T ;

```

1 Initialize  $\mathcal{L}, \mathcal{R} \leftarrow \emptyset, \emptyset$ ;
2  $\mathcal{N} \leftarrow \{T.root\}$ ;
3 while ( $\mathcal{N} \neq \emptyset$ )  $\wedge$  ( $\mathcal{N}[0].depth < d_m$ ) do
4    $N \leftarrow \mathcal{N}.pop(0)$ ;
5    $s \leftarrow \text{ShiftScore}(N, \mathcal{D}_o, \mathcal{D}_u, \mathcal{Q}_o, \mathcal{Q}_u, T)$ ;
6   if ( $s \geq \theta$ ) then
7      $\mathcal{L}.append((OP_N, N))$ ;
8    $\mathcal{N}.append(N.child\_nodes)$ ;
9   if  $\mathcal{N}[0].depth > N.depth$  then
10     $\mathcal{L}.sort(OP_N)$ ;
11    for  $(OP_N, N) \in \mathcal{L}$  do
12      if ( $\text{SpaceRatio}(\mathcal{R} + N) < R_{rc}$ ) then
13         $\mathcal{R}.append(N)$ ;
14     $\mathcal{L} \leftarrow \emptyset$ 
15 return  $\mathcal{R}$ 

```

– 7). If a level of BMTree is evaluated (Line 9), the algorithm sorts \mathcal{L} w.r.t. OP_N (Line 10). Then, if the nodes with greater OS score satisfy the retraining constraint ratio R_{rc} (Line 12), they are added to the retraining nodes list (Line 13).

C. BMTree Reconstruction and Retraining

We proceed to introduce the BMTree reconstruction and retraining procedures. First, we initialize the BMTree w.r.t. the pre-trained BMTree and the BMTree nodes needing retraining that have resulted from the retraining detection procedure.

When the retrain domain (i.e., the to-be-retrained BMTree nodes) is decided, how to retrain the piecewise SFC while maintaining the rest of the designed piecewise SFC portion unchanged is non-trivial. Revisiting the design of seamless partitioning and BMP generation introduced in Section IV, we propose to partially maintain the BMTree structure, and conduct the retraining procedure.

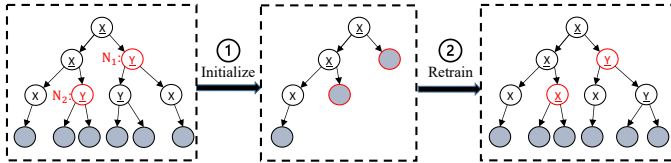


Fig. 7: Partial BMTree retraining procedure.

To conduct the retraining procedure, first, we manipulate the BMTree so that the partial retraining procedure could be finished by regenerating the BMTree structure. As in Fig. 7, suppose N_1 and N_2 are two nodes that represent the subspaces to be retrained. In the initialization of the retraining procedure, we delete the child nodes of N_1 and N_2 as well as the actions assigned to N_1 and N_2 while the other nodes remain unchanged. The BMTree's unchanged portion is in the middle of Fig. 7.

Then, we input the partially deleted BMTree T into an RL environment for retraining. We apply the MCTS method for retraining. Different from the environment introduced for

training the BMTree from scratch (Section V), here the environment is developed to support partially training the BMTree, and is designed as follows:

(1) *State*. We design the state of the retraining RL environment as the nodes to be retrained. In Fig. 7, N_1 and N_2 are initialized in the state: $S = \{(N_1 : \text{None}), (N_2 : \text{None})\}$, where None denotes that no action has been taken yet. (2) *Action*. Then, we design the action space as the actions assigned to N_1 and N_2 . After the action is decided, the child nodes of N_1 and N_2 are generated, and the child nodes of N_1 and N_2 represent the transited state. The nodes of T in one state do not require to have identical depth. (3) *Reward Design*. We apply the updated dataset and query workloads to generate the reward as in Section V. The RL policy training environment will produce a regenerated BMTree noted as T' w.r.t. the redesigned state, action, and reward. Further, to improve efficiency, during the partial retraining procedure, we only generate reward w.r.t. the queries in \mathcal{Q}_u that fall in the retrained nodes.

D. Workflow for Partial Retraining

We summarize the partial retraining procedure as follows: (1) If there exists BMTree node satisfying the shift score filter, the node to retrain detection procedure is conducted (Alg. 1). Then, the retraining RL environment is initialized and the BMTree is regenerated based on the updated data and query. Particularly, if the retraining result does not meet expectation (e.g., with optimization ratio less than 1%), the procedure will select and retrain more untrained nodes as in Section VI-C.

Algorithm 2: BMTree Structure Partial Retraining.

input : n -dimensional old and updated datasets $\mathcal{D}_o, \mathcal{D}_u$, old and updated training workloads $\mathcal{Q}_o, \mathcal{Q}_u$, BMTree T ;
output : Retrained BMTree T' ;

```

1 if  $\exists N \in T$  with  $\text{shift}_m(N) \geq \theta_s$  then
2    $\mathcal{R} \leftarrow \text{Retrain\_Detector}(T, \mathcal{D}_o, \mathcal{D}_u, \mathcal{Q}_o, \mathcal{Q}_u)$ ;
3    $S, T_p = \text{Initial}(\mathcal{R}, T)$ ;
4    $\mathcal{Q}'_u \leftarrow \{q | q \in \mathcal{Q}_u \wedge \exists N \text{ s.t. } N \text{ contains } q\}$ ;
5    $T' \leftarrow \text{MCTS}(T_p, \mathcal{D}_u, \mathcal{Q}'_u)$ ;
6 if limited optimization then Retrain  $T'$ ;
7 return  $T'$ 

```

The pseudo-code of the retraining procedure is given in Alg. 2. If there exists a BMTree node that satisfy the shift score requirement (Line 1), it first detects the BMTree nodes to be retrained (Line 2). Then, the RL retrain environment, the partially deleted BMTree T_p , and the initial state for RL training are initialized (Line 3), and the queries contained by the to-be-retrained BMTree nodes are selected for retraining (Line 4). The MCTS algorithm with the environment redesigned as above is applied to regenerate the BMTree w.r.t. the updated database and the query workload (Line 5). If T' has limited performance enhancement, when T' optimizes ScanRange by less than 1% improvement compared with the original T (Line 6).

After retraining the BMTree nodes is complete, data is needed to update the SFC values. With BMTree being partially retrained, only the data located in the retrained subspaces

TABLE I: Experiment Parameters.

Parameter	Value
Data	GAU UNI OSM-US TIGER
Query	GAU SKE UNI
Sampling rate	0.01 0.025 0.05 0.075 0.1
# Training Q	100 500 1000 1500 2000
Max depth	1 5 10 15 20

should be updated. The retraining procedure also reduces the cost of the following index update procedure.

VII. ANALYSIS AND DISCUSSION

Injection and Monotonicity. We prove that piecewise SFCs modeled by the BMTree satisfy both injection and monotonicity properties. The proof is detailed in [29].

Time Complexity Analysis. We provide time complexities for SFC value computation and MCTS-based BMTree construction. The time complexity for computing the SFC value of \mathbf{x} using the constructed BMTree is $O(M)$, where M is the length of $C_T(\mathbf{x})$. This complexity is comparable to other SFCs described by BMPs. For BMTree construction, the complexity of the MCTS BMTree construction is $O(M \cdot (N + |\mathcal{D}_s| (M + \log |\mathcal{D}_s|) + |\mathcal{Q}|))$, where N is the child node size of the policy tree, $|\mathcal{D}_s|$ and $|\mathcal{Q}|$ correspond to the size of the sampled data and query workloads. It takes at most M actions to construct the BMTree. In each step of choosing an action, the selection step is bounded by the child node size $O(N)$; the simulation time corresponds to the computation of ScanRange that takes $O(M \cdot |\mathcal{D}_s|)$ for SFC value computing, $O(|\mathcal{D}_s| \cdot \log(|\mathcal{D}_s|))$ to sort data, and $O(|\mathcal{Q}|)$ to compute ScanRange for each query. For BMTree update, suppose the BMTree construction complexity is noted as $T(\text{BMT_Train})$. The BMTree retraining time is bounded by $R_{rc} \cdot T(\text{BMT_Train})$ with R_{rc} as the retraining constraint ratio, since the ratio will limit the retrain nodes and the depth of the BMTree that needs to be generated by the MCTS algorithm.

VIII. EVALUATION

Experiments aim to evaluate the following: (1) The effectiveness of BMTree’s design, including (i) Evaluating the proposed piecewise SFC method vs. existing SFCs when applied to the SFC-based indexes vs. the other indexes, (ii) The BMTree under different settings (e.g., scalability, dimensionality, and aspect ratio), and (iii) Components of the BMTree by evaluating different BMTree variants. (2) The effectiveness of partial retraining, including (i) Evaluating the performance of partial retraining while varying distribution shift settings, and (ii) Evaluating the choice of parameters, e.g., the retraining constraint and the shift score threshold study during partial retraining.

A. Experimental Setup

Dataset. We conduct experiments on both synthetic and real datasets. For synthetic datasets, we generate data points in the two-dimensional data space with a granularity size of $2^{20} \times 2^{20}$ that follow either uniform (denoted as UNI) or Gaussian distributions (denoted as GAU) with μ_d as the center

point of the space domain. Real data OSM-US contains about 100 Million spatial objects in the U.S. extracted from OpenStreetMap API [37], and TIGER [38] contains 2.3 Million water areas in North America cleaned by SpatialHadoop [39]. **Query Workload.** We follow [24, 12] to generate query workloads. We generate various types of window queries, where each query type has a fixed area selected from $\{2^{30}, 2^{32}, 2^{34}\}$ and a fixed aspect ratio selected from $\{4, 1, 1/4\}$; Each workload comprises multiple query types with different combinations of areas and ratios. We generate queries with Uniform (UNI) and Gaussian (GAU) distributions (same as in [4, 12]), We also generate a skewed workload (denoted by SKE), in which queries follow Gaussian distributions with different μ values.

Index Structures. To evaluate the performance of the proposed piecewise SFC compared with the existing SFCs, we integrate the proposed piecewise SFC and the baseline SFCs into both traditional indexes and learned index structures. First, we integrate the piecewise SFC (and baseline SFCs) into the PostgreSQL database system and a built-in B^+ -Tree variant in PostgreSQL is employed with SFC values as key values. Second, we use a learned spatial index, RSMI [40], to compare the performance of the piecewise SFC against the baseline SFCs within RSMI. The B^+ -Tree of PostgreSQL is a disk-based index while the released implementation of RSMI [40] is memory based. We choose them to evaluate the performance of the piecewise SFC under various scenarios.

SFC Baselines. We choose the following SFC methods as our baselines: (1) Z-curve [20, 30]; (2) Hilbert Curve [21]; (3) QUILTS [24].

Evaluation Metrics. For experiments conducted with PostgreSQL, we use the I/O cost (I/O) recorded by PostgreSQL and the Query Latency (QL). For experiments under RSMI, we report the number of node accesses of its tree structure and QL for a fair comparison by following [40, 41].

Parameter Settings. Table I lists the parameters used in our experiments, and the default settings are in bold. We set the number of rollouts (as described in Section V) in MCTS at 10 by default. The max depth is the depth of the BMTree built via the RL model; the sampling rate (0.05 by default) is the rate of sampling training data for computing the ScanRange. **Evaluation Platform.** We train the BMTree with PyTorch 1.9, Python 3.8. The experiments are conducted on an 80-core server with an Intel(R) Xeon(R) Gold 6248 CPU@2.50GHz 64.0GB RAM, no GPU resource is leveraged.

B. Evaluation of the BMTree

1) Effectiveness: This experiment is to compare the effectiveness of the learned piecewise SFC in query processing against the other SFCs under both the PostgreSQL and the RSMI environments. We also compare an SFC-based index combined with the BMTree against the other indexes. For each experiment, we use 1000 windows queries, which are randomly generated by following respective distributions for training, and another 2000 different window queries following the same distribution for evaluation.

Results on PostgreSQL. Figures 8a and 8b show the I/O and QL on window queries. To ensure PostgreSQL conducts

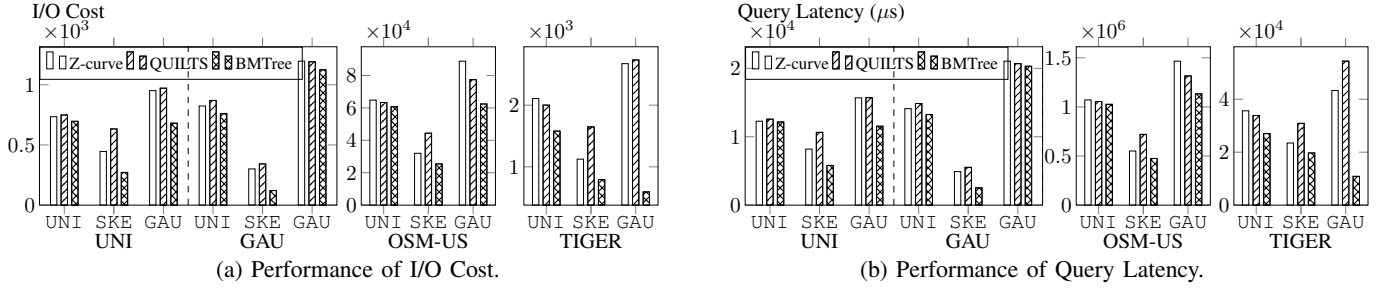


Fig. 8: Results under PostgreSQL, where the first and the second lines under the x bar denote the query and data distribution.

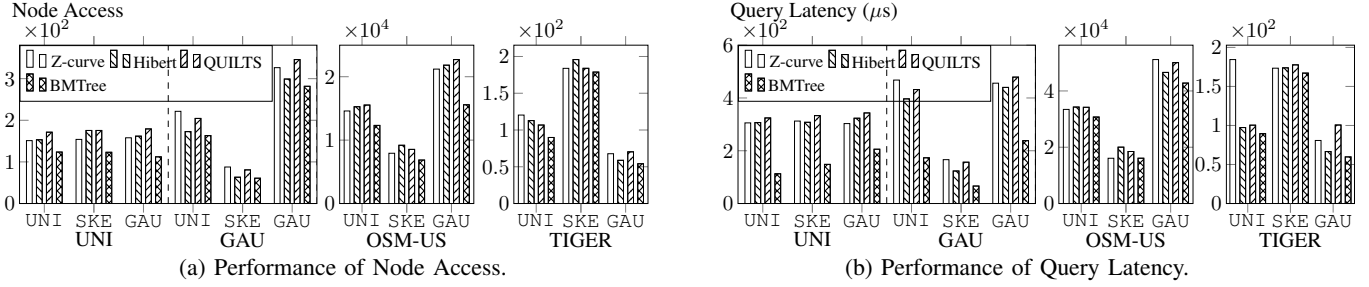


Fig. 9: Results using RSMI learned index structure.

indexscan during querying, both the bitmapscan and seqscan in PostgreSQL are disabled. We do not include the Hilbert curve for this experiment as the Hilbert curve requires additional structure and dedicated algorithm for returning accurate results for window queries, and PostgreSQL does not support them for the Hilbert curve.

Observe that the proposed BMTree consistently outperforms the baselines in all the combinations of data and query distributions in terms of both I/O and QL. Between the two baselines, QUILTS performs worse for the SKE workload, and performs similarly as the Z-curve for UNI and GAU workloads. The reason is that our query workload contains queries with different aspect ratios (e.g., 4 and 1/4), rather than queries with similar aspect ratios as it is used in QUILTS [24]. QUILTS can only choose queries with a particular aspect ratio to optimize, and this results in poor performance for queries with different aspect ratios. The BMTree outperforms the Z-curve by 5.2%–39.1% (resp. 7.7%–59.8%, 6.3%–29.8% and 25.1%–77.8%) in terms of I/O on UNI (resp. GAU, OSM-US, and TIGER) datasets across the various workloads. The results in terms of QL are consistent with those of I/O. BMTree’s superior performance is because (1) The BMTree generates piecewise SFCs to handle distinct query distributions, and (2) The BMTree is equipped with effective learning to generate BMPs and subspaces. Notice that under the UNI workload, the BMTree outperforms the Z-curve by 25.1% on TIGER while it only outperforms Z-curve slightly on the other three datasets. This is expected: Under the UNI query workload, the BMTree can only make use of the data but not the query distributions to optimize performance; TIGER is very skewed and the BMTree can capture TIGER’s skewed data nature.

Results on RSMI. The original RSMI [12] uses the Hilbert curve, and we include it as a baseline for this experiment as RSMI returns approximate results for all curves. All the curves achieve comparable recall (99.5% or above) using RSMI’s

algorithms for window queries. Figures 9a and 9b show the number of node accesses and QL for all curves when using RSMI. Observe that the BMTree consistently outperforms all baselines. The BMTree outperforms the Z-curve by 18.2%–29.0% (resp. 13.7%–28.4%, 13.5%–26.5%, and 2.8%–25.3%) in terms of the number of node accesses on the UNI (resp. GAU, US-OSM, and TIGER) datasets. Also, observe that the Hilbert curve achieves similar performance to that of the BMTree on the GAU dataset that could be attributed to its good tolerance to data skew [42].

Comparison with Other Indexes. We compare against the performance of two SFC-based indexes, RSMI and ZM combining our BMTree, with baseline indexes including (1) two R-tree variants: STR [43] and R* Tree [44]; and (2) two partition-based methods: Grid-File and Quad-Tree. The results are given in [29] that reveal the generality of the BMTree on enhancing query performance combining different indexes.

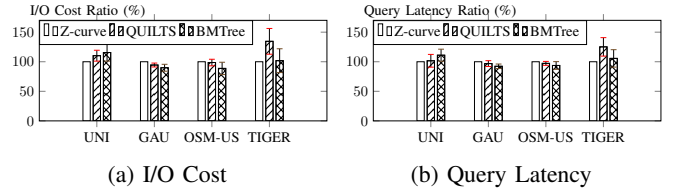


Fig. 10: Performance of k NN queries.

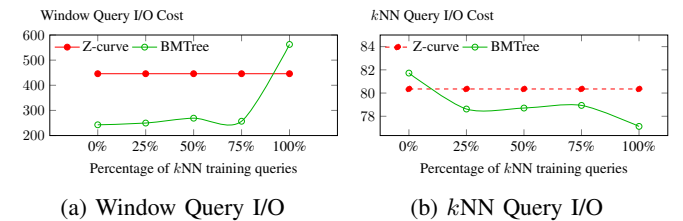


Fig. 11: Optimization of window query & k NN query.

Effect on k NN Queries. The piecewise SFC is learned to optimize window queries. Here, we investigate its influence on the performance of k NN queries. We generate 1,000 k NN query points following the data distribution, and we apply the k NN algorithm [12] in PostgreSQL with k set to 25. We report the I/O and QL ratios in Figure 10a and 10b that are the ratio of results of the different curves divided by the result of the Z-curve. The BMTree performs slightly better than the baselines on GAU and OSM-US while the Z-curve is slightly better on UNI and TIGER. Thus, while the piecewise SFC is optimized for window queries, its k NN query performance is not compromised.

Optimizing Window and k NN queries. We evaluate the performance when window queries and k NN queries are optimized together. To optimize the BMTree for k NN queries, we convert k NN queries into window queries by following [12] and include them in the training workload. Then, we vary the weight of the objective based on k NN queries relative to window queries from 0% to 100% during training. Figures 11a and 11b give the window and k NN query I/Os. Observe that as the weight increases, the window query I/O tends to increase while the k NN query I/O tends to decrease. Also, observe that when the weight is between 25% and 75%, the performance of the window query only mildly degrades, while the performance of k NN query is better than that based on the Z-curve. The results show the potential of the BMTree to optimize the two query types together.

2) *Effect of Varying the Settings:* We evaluate the performance of the BMTree under various settings: dataset/query size, dimensionality, and window aspect ratio. More settings can be found in [29].

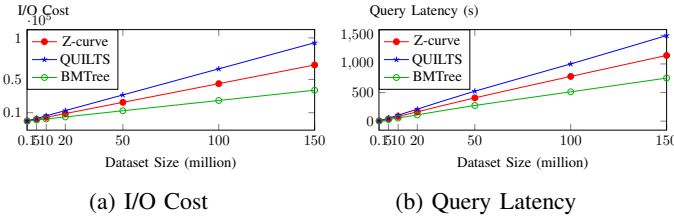


Fig. 12: Performance vs dataset size.

Scalability of the Learned SFCs. To evaluate the scalability of the BMTree, we evaluate the performance of the SFCs by varying data size from 0.1 to 150 Million. We construct the BMTree using 10^5 sampled data points as input for RL training and the others follow the default settings. The results are in Figure 12. Observe that the BMTree displays a linear trend for both I/O and QL when data size increases. We observe similar trends for baselines.

Effect of Higher Dimensionality. To evaluate the effect of dimensionality on the effectiveness of the learned SFC, we vary the dimensionality from 2 to 6 on the datasets for both the uniform and normal distributions. We report the IO in Figure 13. The BMTree consistently outperforms the baselines, and saves up to 54% of the I/O cost compared to the best Z-curve baseline. This demonstrates that the BMTree generalizes well on data with more than two dimensions.

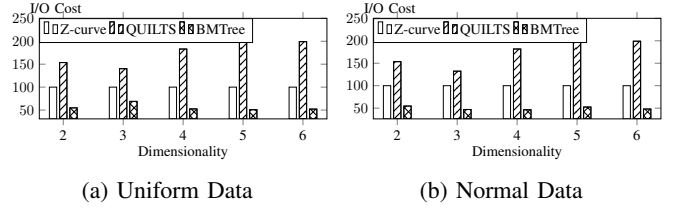


Fig. 13: I/O cost vs dimensionality.

Effect of Varying Query Aspect Ratio and Selectivity.

(1) We evaluate the BMTree performance by varying query aspect ratios from $\{4, \frac{1}{4}\}$ to $\{128, \frac{1}{128}\}$, and the results are reported in Figure 14a. Observe that the BMTree performs consistently better than the other SFCs across different aspect ratios including very wide ones. (2) We vary query selectivity from 0.0001% to 1%, and report the results in Figure 14b. Observe that the improvement of the BMTree is subtle under very small query range. This is due to the fact that for small query ranges, the points that are within a range are few, and the index tends to perform similarly for different SFCs.

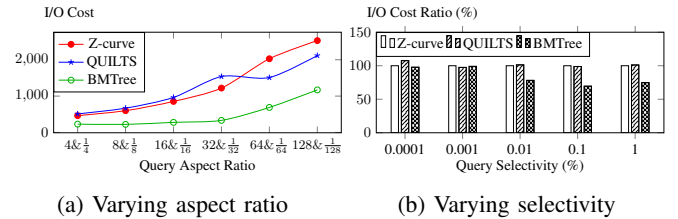


Fig. 14: Varying query aspect ratio and selectivity.

3) *Evaluating BMTree Variants:* We study 4 BMTree variants: BMTree-Data Driven (with dataset only), BMTree-noGAS (with no GAS algorithm), BMTree-greedy (pure greedy), and BMTree-LMT (with limited BMPs). Results are in Figure 15. (1) **BMTree-DD.** We evaluate the BMTree

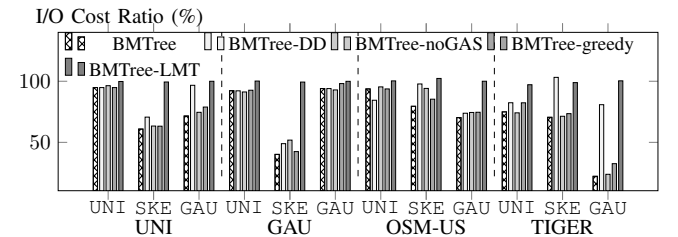


Fig. 15: I/O Cost on BMTree Variants.

performance when the query workload is not available. We generate training queries for the BMTree by following the dataset's distribution. From Figure 15, observe that BMTree-DD performs comparable to the BMTree on the UNI workloads for all datasets. However, on the SKE workload, the BMTree performs generally much better. (2) **BMTree-noGAS.** We evaluate the effectiveness of the GAS algorithm. Observe the performance drop compared to the MCTS using GAS. This shows the effect of GAS. (3) **BMTree-greedy.** We apply GAS for all action selections, and build a purely greedy based BMTree. Observe that MCTS with GAS outperforms both BMTree-noGAS and BMTree-greedy. This indicates a

synergistic improvement of MCTS over GAS. **(4) BMTree-LMT.** We consider all BMPs, and design a baseline BMTree where only the Z- and C-curves are allowed to be assigned to the subspaces. We observe a significant improvement in the BMTree over using the Z- and C-curves alone. This demonstrates the necessity of considering all BMPs.

C. Effectiveness of Partial Retraining of the BMTree

1) *Varying Distribution Shift Settings:* We evaluate the effectiveness of our proposed partial retraining mechanism. Specifically, we evaluate three situations: data shift while the queries are fixed, query shift while the data is fixed, and the composed scenario. We compare three methods: (1) Keeping the original BMTree unchanged (noted as BMT-O), (2) Fully retrained BMTree (noted as BMT-FR), and (3) Partially retrained BMTree (noted as BMT-PR). We restrict the partial retrain constraint ratio to 0.5, where at most half of the space area can be retrained. Also, we evaluate the performance while varying the retrain constraints.

Evaluation of Data Shift. We evaluate 3 different metrics: the I/O Cost and Query Latency of the constructed BMTree, and the training time needed to retrain the BMTree. The data shifts from the GAU to the UNI distribution. The results are in Fig. 16. In Fig. 16a, the partially retrained BMTree BMT-PR achieves a performance increase on I/O cost compared to the original BMTree BMT-O, while optimizing the percentage from 9.2% to 12.1% and varying the shift percentage. Compared to the fully retrained BMTree BMT-FR, BMT-PR achieves an average of 90.6% performance improvement achieved by BMT-FR. Under a 90% data shift, BMT-PR outperforms BMT-FR and achieves over $2.3\times$ reduction in I/O cost compared with BMT-FR. The reason is that BMT-PR allows the agent to focus on optimizing the subspace with vital distribution changes, which allows for the partially retrained BMTree to achieve a better performance on this focused subspace. The results of the query latency are generally consistent with the results of I/O Cost, in which BMT-PR achieves an average of 91.7% performance improvement achieved by BMT-FR, as in Fig. 16b.

As for the training time (Fig. 16c), BMT-FR costs from 7857s to 8314s (8125.5s on average) to retrain the BMTree from scratch, while BMT-PR costs from 559.2s to 3778.8s (1833.3s on average). BMT-PR achieves approximately $4.4\times$ reduction of training time compared with BMT-FR, that is aligned with the time complexity estimation, where with a retraining constraint ratio of R_{rc} , the training time of BMT-PR is upper bounded by $R_{rc} \cdot \text{time}(\text{BMT-PR})$.

Evaluation of Query Shift. We proceed to evaluate the effect of query workload shift. Under the GAU data, we shift the distribution of the query workload. Specifically, we vary the μ values of the Gaussian distributions of queries, and generate 2 skew query workloads, namely SKE₁ and SKE₂, respectively. The query workload is shifted from SKE₁ to SKE₂. We estimate the retrain performance by varying the shift percentage. The results are in Fig. 17. Both the fully and partially retrained BMTrees BMT-FR and BMT-PR have limited optimization compared to the original BMTree (less than 1% on I/O Cost) before the shift reaches 50% percentage. However, when

the shift percentage reaches 70%, the optimizing potential becomes vital. BMT-PR reduces I/O Cost from 7.3% to 16.7% compared with the BMT-O. We observe that BMT-PR achieves better performance on I/O Cost compared with BMT-FR from shift percentage 70% to 90% (over $1.8\times$ at 90%). This reveals that retraining a subspace with a significant change in query workload may significantly enhance performance compared with training a BMTree for the whole data space. The query latency results are similar in I/O Cost (as in Fig. 17b) that is consistent with the data shift situation.

The training time (Fig. 17c) also aligns with the time complexity evaluation. BMT-FR spends from 7295.5s to 8485.8s (on average, 7716.9s) to retrain the BMTree, while BMT-PR spends from 255.9s to 1571.1s (on average, 1237.1s), achieves approximately over $6.2\times$ reduction in training time.

Evaluation of Mixed Shift of Data and Query. We evaluate the scenario when both data and query shift, and the shift settings of data and query follow the former experiments. We select shift percentages from: {25%, 50%, 75%} for both data and query. The results are in Fig. 18. The partially retrained BMTree BMT-PR achieves different levels of optimizations when varying data and query shift percentages. BMT-PR achieves remarkable I/O Cost reduction when query or data shift reaches 75% (the 3rd row and the 3rd column in Fig. 18 denote when data and query shift reaches 75%, respectively), which achieves on average 8.3% (resp. 16.5%) reduction in I/O cost under 75% data shift (resp. query shift) compared with BMT-O. BMT-PR outperforms BMT-FR in certain cases (e.g., $25\% \times 25\%$ data-query shift), and achieves competitive performance in the majority of situations. BMT-PR remains efficient compared with BMT-FR on training time. Particularly, under 50% query shift, the training time reduction of BMT-PR is less than $2\times$ compared with BMT-FR. Observe that the second partial retraining is triggered since the first partial retraining does not achieve notable optimization. Compared with BMT-FR, a full retraining is preferred as the action in the root node of the BMTree needs to be modified.

2) *Varying the Retraining Hyperparameters:* We evaluate how the retraining hyperparameters affect I/O Cost. We consider the retraining constraint ratio and the shift score threshold. We conduct the hyperparameter estimations under $75\% \times 75\%$ data and query shifts. The results are in Fig. 19.

(1) The Retraining Constraint Ratio R_{rc} . We vary R_{rc} from 0.1 to 1 to study how R_{rc} affects the retraining performance. As in Fig. 19a, BMT-PR achieves almost no performance enhancement compared to BMT-O, as the very small retraining constraint ratios (0.1 and 0.2) limit the ability of the retrain method to retrain the important nodes that do not satisfy the constraint. BMT-PR achieves optimal performance with a constraint ratio of 0.5 that allows retraining nodes that mostly affect query performance.

(2) The Shift Score Threshold. We vary the shift score threshold from 0.1 to 0.5. As in Fig. 19b, observe that the threshold from 0.1 to 0.35, BMT-PR has similar performance compared to a full retrain. When the threshold is 0.4 and above, it filters nodes that achieve notable performance improvement (with threshold lower than 0.4) and become ineffective. This identifies the best choices for the shift score threshold.

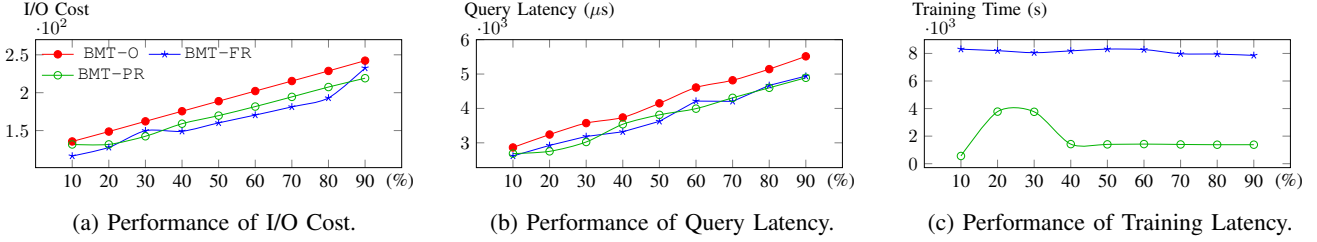


Fig. 16: Evaluation of data shift while fixing the queries. The data is shifted from a GAU to UNI with varying UNI percentage from 10% to 90%.

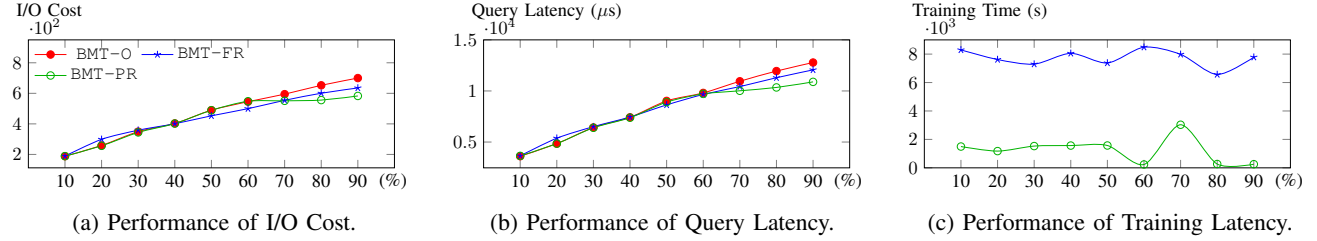


Fig. 17: Query shift while fixing the data. Query workload is shifted from 10% to 90% of the new query workload.

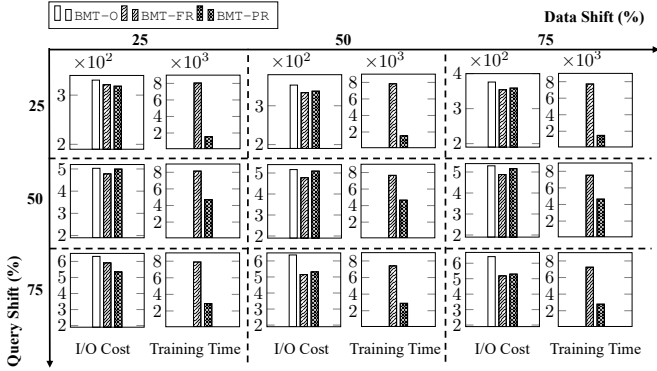


Fig. 18: Evaluation of mixed shift of data and query.

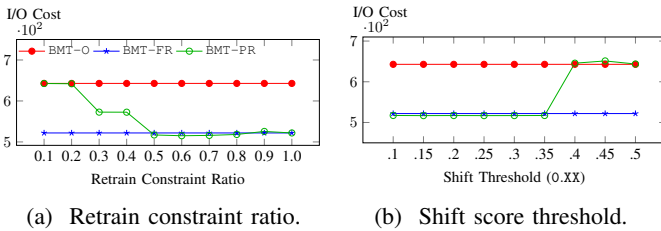


Fig. 19: Varying retrain constraint ratio & shift score threshold.

IX. RELATED WORK

Space-Filling Curves (SFCs). Many SFCs have been developed. The C-curve [19] organizes the data points dimension at a time. The Z and Hilbert curves [16, 17, 18, 19, 20, 21, 22] are widely used in index design. Despite the success of these SFCs, they do not consider data and query workload distributions. QUILTS [24] is proposed to consider data and query distributions in designing the mapping function of SFCs. All these SFCs, including QUILTS, adopt a single mapping scheme that may not always be suitable for the

whole data space and query workload (Section I). This paper proposes the first piecewise SFC that uses different mapping functions for the different data subspaces. It considers both data and query distributions. Furthermore, we propose a reinforcement learning-based method to learn SFCs to directly optimize performance. Following the BMTree [29], there is work [45, 46] that leverages learning to construct SFCs. The proposed piecewise SFC design potentially extends the design space of SFCs. Moreover, these studies do not consider fast updating of SFCs. This paper proposes partially regenerating the BMTree, which reduces the update cost and only requires part of the data to update the SFC values.

SFC-based Index Structures. SFCs are used for indexing multi-dimensional data, and is widely adopted by DBMSs. Also, SFCs are essential for learned multi-dimensional indexes (e.g., [11, 12, 47]). ZM [11] combines a Z-curve with a learned index, namely RMI [2]. RSMI [12] applies the Hilbert curve together with a learned index structure for spatial data. Pai et al. [48] present preliminary results on the instance-optimal Z-index based on the Z-curve that adapts to data and workload. SFC-based indexes can also be applied for data skipping [49, 50, 51] that aim to partition and organize data into data pages so that querying algorithms only access pages that are relevant to a query. An SFC-based approach [15] maps multidimensional points to scalar values using an SFC, and uses the B⁺-Tree or range-partitioned key-value store (e.g., H-base) for partitioning and organizing data.

Analysis of SFCs. Many studies, e.g., [52, 20, 53, 21, 42, 24] evaluate SFCs. Mokbel et al. [52, 20, 53] discuss the characteristics of good SFCs. Moon et al. [21] propose the number of disk seeks during query processing. Xu et al. [42] prove that the Hilbert curve is a preferable SFC from that respect. Nishimura et al. [24] propose a *cohesion* cost that evaluates how good SFCs cluster data. Recently, Liu et al. [46] propose a cost model that evaluates query performance of SFCs. It uses the BMTree and speedups reward computing.

Reinforcement Learning (RL) in Indexing. Our method of

generating SFCs is based on RL techniques [54, 27]. There are several recent studies, e.g., [51, 55, 41] on applying RL to generate tree structures. Yang et al. [51] construct the Qd-tree for partitioning data into blocks on storage with Proximal Policy Optimization networks (PPO) [34]. Gu et al. [41] utilize RL to construct the R-tree for answering spatial queries [17], and Neurocuts [55] constructs a decision tree using a RL agent. These RL designs are not suitable for learning piecewise SFCs. Our design of RL models is based on MCTS and is different from the designs in these studies.

X. CONCLUSION

In this paper, we study the Space-Filling Curve Design problem, and propose constructing piecewise SFCs that adopt different mapping schemes for different data subspaces. Specifically, we propose the BMTree for maintaining multiple bit merging patterns in which every path corresponds to a BMP. We propose to construct the BMTree in a data-driven manner via reinforcement learning. Further, we develop a partial re-training procedure that supports retraining parts of the BMTree while retaining the rest unchanged instead of training from scratch. We conduct extensive experiments on both synthetic and real datasets with various query workloads. Experiments show that the piecewise SFCs are consistently superior over existing SFCs, especially when data and/or queries have a certain degree of skewness.

REFERENCES

- [1] R. Bayer, “The universal b-tree for multidimensional indexing: general concepts,” in *Worldwide Computing and Its Applications, International Conference*, ser. Lecture Notes in Computer Science, vol. 1274. Springer, 1997, pp. 198–209.
- [2] T. Kraska, A. Beutel, E. H. Chi, J. Dean, and N. Polyzotis, “The case for learned index structures,” in *ACM SIGMOD*, 2018, pp. 489–504.
- [3] J. Ding, U. F. Minhas, J. Yu, C. Wang, J. Do, Y. Li, H. Zhang, B. Chandramouli, J. Gehrke, D. Kossmann, D. B. Lomet, and T. Kraska, “ALEX: an updatable adaptive learned index,” in *ACM SIGMOD*, 2020, pp. 969–984.
- [4] J. Ding, V. Nathan, M. Alizadeh, and T. Kraska, “Tsunami: A learned multi-dimensional index for correlated data and skewed workloads,” *Proc. VLDB Endow.*, vol. 14, no. 2, pp. 74–86, 2020.
- [5] R. Marcus, A. Kipf, A. van Renen, M. Stoian, S. Misra, A. Kemper, T. Neumann, and T. Kraska, “Benchmarking learned indexes,” *Proc. VLDB Endow.*, vol. 14, no. 1, pp. 1–13, 2020.
- [6] C. Faloutsos, “Gray codes for partial match and range queries,” *IEEE Trans. Software Eng.*, vol. 14, no. 10, pp. 1381–1393, 1988.
- [7] C. Faloutsos and S. Roseman, “Fractals for secondary key retrieval,” in *Proceedings of the Eighth ACM SIGACT-SIGMOD-SIGART Symposium on Principles of Database Systems*, 1989, pp. 247–252.
- [8] K. C. K. Lee, W. Lee, B. Zheng, H. Li, and Y. Tian, “Z-SKY: an efficient skyline query processing framework based on z-order,” *VLDB J.*, vol. 19, no. 3, pp. 333–362, 2010.
- [9] M. L. Yiu, Y. Tao, and N. Mamoulis, “The B^{dual} -tree: indexing moving objects by space filling curves in the dual space,” *VLDB J.*, vol. 17, no. 3, pp. 379–400, 2008.
- [10] L. Zhou, C. R. Johnson, and D. Weiskopf, “Data-driven space-filling curves,” *IEEE Trans. Vis. Comput. Graph.*, vol. 27, no. 2, pp. 1591–1600, 2021.
- [11] H. Wang, X. Fu, J. Xu, and H. Lu, “Learned index for spatial queries,” in *20th IEEE International Conference on Mobile Data Management*, 2019, pp. 569–574.
- [12] J. Qi, G. Liu, C. S. Jensen, and L. Kulik, “Effectively learning spatial indices,” *Proc. VLDB Endow.*, vol. 13, no. 11, pp. 2341–2354, 2020.
- [13] n.d., “Postgis,” https://postgis.net/docs/using_postgis_dbmanagement.html, 2023, [Online; accessed 3-May-2023].
- [14] Z. Slayton, “Z-order indexing for multifaceted queries in amazon dynamodb,” <https://aws.amazon.com/blogs/database/>, 2017.
- [15] S. Nishimura, S. Das, D. Agrawal, and A. E. Abbadi, “Md-hbase: A scalable multi-dimensional data infrastructure for location aware services,” in *12th IEEE International Conference on Mobile Data Management*. IEEE Computer Society, 2011, pp. 7–16.
- [16] J. A. Orenstein and T. H. Merrett, “A class of data structures for associative searching,” in *Proceedings of the Third ACM SIGACT-SIGMOD Symposium on Principles of Database Systems*, 1984, pp. 181–190.
- [17] J. A. Orenstein, “Spatial query processing in an object-oriented database system,” in *ACM SIGMOD*, 1986, pp. 326–336.
- [18] —, “Redundancy in spatial databases,” in *ACM SIGMOD*, 1989, pp. 295–305.
- [19] H. V. Jagadish, “Linear clustering of objects with multiple attributes,” in *ACM SIGMOD*, 1990, pp. 332–342.
- [20] M. F. Mokbel, W. G. Aref, and I. Kamel, “Analysis of multi-dimensional space-filling curves,” *GeoInformatica*, vol. 7, no. 3, pp. 179–209, 2003.
- [21] B. Moon, H. V. Jagadish, C. Faloutsos, and J. H. Saltz, “Analysis of the clustering properties of the hilbert space-filling curve,” *IEEE Trans. Knowl. Data Eng.*, vol. 13, no. 1, pp. 124–141, 2001.
- [22] A. Kipf, H. Lang, V. Pandey, R. A. Persa, C. Anneser, E. T. Zacharitou, H. Doraiswamy, P. A. Boncz, T. Neumann, and A. Kemper, “Adaptive main-memory indexing for high-performance point-polygon joins,” pp. 347–358, 2020.
- [23] H. Samet, *Foundations of multidimensional and metric data structures*, ser. Morgan Kaufmann series in data management systems, 2006.
- [24] S. Nishimura and H. Yokota, “QUILTS: multidimensional data partitioning framework based on query-aware and skew-tolerant space-filling curves,” in *ACM SIGMOD*, 2017, pp. 1525–1537.
- [25] K. C. K. Lee, B. Zheng, H. Li, and W. Lee, “Approaching

- the skyline in Z order,” in *Proceedings of the 33rd International Conference on Very Large Data Bases*. ACM, 2007, pp. 279–290.
- [26] M. L. Puterman, *Markov Decision Processes: Discrete Stochastic Dynamic Programming*, ser. Wiley Series in Probability and Statistics, 1994.
- [27] C. Browne, E. J. Powley, D. Whitehouse, S. M. Lucas, P. I. Cowling, P. Rohlfshagen, S. Tavener, D. P. Liebana, S. Samothrakis, and S. Colton, “A survey of monte carlo tree search methods,” *IEEE Trans. Comput. Intell. AI Games*, vol. 4, no. 1, pp. 1–43, 2012.
- [28] J. Lu, A. Liu, F. Dong, F. Gu, J. Gama, and G. Zhang, “Learning under concept drift: A review,” *IEEE Trans. Knowl. Data Eng.*, vol. 31, no. 12, pp. 2346–2363, 2018.
- [29] J. Li, Z. Wang, G. Cong, C. Long, H. M. Kiah, and B. Cui, “Towards designing and learning piecewise space-filling curves,” *Proceedings of the VLDB Endowment*, vol. 16, no. 9, pp. 2158–2171, 2023.
- [30] T. Skopal, M. Krátký, J. Pokorný, and V. Snásel, “A new range query algorithm for universal b-trees,” *Inf. Syst.*, vol. 31, no. 6, pp. 489–511, 2006.
- [31] G. Peano, “Sur une courbe, qui remplit toute une aire plane,” *Mathematische Annalen*, vol. 36, no. 1, pp. 157–160, 1890.
- [32] J. K. Lawder and P. J. H. King, “Querying multi-dimensional data indexed using the hilbert space-filling curve,” *SIGMOD Rec.*, vol. 30, no. 1, pp. 19–24, 2001.
- [33] B. Fuglede and F. Topsøe, “Jensen-shannon divergence and hilbert space embedding,” in *Proc. IEEE ISIT*. IEEE, 2004, p. 31.
- [34] J. Schulman, F. Wolski, P. Dhariwal, A. Radford, and O. Klimov, “Proximal policy optimization algorithms,” *CoRR*, vol. abs/1707.06347, 2017.
- [35] X. Zhou, G. Li, C. Chai, and J. Feng, “A learned query rewrite system using monte carlo tree search,” *Proc. VLDB Endow.*, vol. 15, no. 1, pp. 46–58, 2021.
- [36] L. Kocsis and C. Szepesvári, “Bandit based monte-carlo planning,” in *Machine Learning: ECML 2006, 17th European Conference on Machine Learning*, ser. Lecture Notes in Computer Science, vol. 4212. Springer, 2006, pp. 282–293.
- [37] “Openstreetmap,” <http://www.openstreetmap.org/>, 2023, [Online; accessed 3-May-2023].
- [38] “Tiger/line shapefiles,” <https://www.census.gov/geographies/mapping-files/time-series/geo/tiger-line-file.html>, 2022, [Online; accessed 3-May-2023].
- [39] A. Eldawy and M. F. Mokbel, “Spatialhadoop: A mapreduce framework for spatial data,” in *IEEE ICDE*, 2015, pp. 1352–1363.
- [40] G. Liu, “Released RSMI Code,” <https://github.com/Liuguanli/RSMI>, 2020.
- [41] T. Gu, K. Feng, G. Cong, C. Long, Z. Wang, and S. Wang, “The rlr-tree: A reinforcement learning based r-tree for spatial data,” *ACM SIGMOD*, vol. 1, no. 1, pp. 1–26, 2023.
- [42] P. Xu and S. Tirthapura, “Optimality of clustering properties of space-filling curves,” *ACM Trans. Database Syst.*, vol. 39, no. 2, pp. 10:1–10:27, 2014.
- [43] S. T. Leutenegger, J. M. Edgington, and M. A. López, “STR: A simple and efficient algorithm for r-tree packing,” in *ICDE*, 1997, pp. 497–506.
- [44] N. Beckmann, H. Kriegel, R. Schneider, and B. Seeger, “The r*-tree: An efficient and robust access method for points and rectangles,” in *ACM SIGMOD*, 1990, pp. 322–331.
- [45] J. Gao, X. Cao, X. Yao, G. Zhang, and W. Wang, “Lmsfc: A novel multidimensional index based on learned monotonic space filling curves,” *Proceedings of the VLDB Endowment*, vol. 16, no. 10, pp. 2605–2617, 2023.
- [46] G. Liu, L. Kulik, C. S. Jensen, T. Li, and J. Qi, “Efficient cost modeling of space-filling curves,” *arXiv preprint arXiv:2312.16355*, 2023.
- [47] Z. Zhang, P. Jin, X. Wang, Y. Lv, S. Wan, and X. Xie, “COLIN: A cache-conscious dynamic learned index with high read/write performance,” *J. Comput. Sci. Technol.*, vol. 36, no. 4, pp. 721–740, 2021.
- [48] S. G. Pai, M. Mathioudakis, and Y. Wang, “Towards an instance-optimal z-index,” in *4th International Workshop on Applied AI for Database Systems and Applications (AIDB@ VLDB2022)*, 2022.
- [49] V. Raman, G. K. Attaluri, R. Barber, N. Chainani, D. Kalmuk, V. KulandaiSamy, J. Leenstra, S. Lightstone, S. Liu, G. M. Lohman, T. Malkemus, R. Müller, I. Pandis, B. Schiefer, D. Sharpe, R. Sidle, A. J. Storm, and L. Zhang, “DB2 with BLU acceleration: So much more than just a column store,” *Proc. VLDB Endow.*, vol. 6, no. 11, pp. 1080–1091, 2013.
- [50] L. Sun, M. J. Franklin, S. Krishnan, and R. S. Xin, “Fine-grained partitioning for aggressive data skipping,” in *ACM SIGMOD*. ACM, 2014, pp. 1115–1126.
- [51] Z. Yang, B. Chandramouli, C. Wang, J. Gehrke, Y. Li, U. F. Minhas, P. Larson, D. Kossmann, and R. Acharya, “Qd-tree: Learning data layouts for big data analytics,” in *ACM SIGMOD*, 2020, pp. 193–208.
- [52] M. F. Mokbel and W. G. Aref, “Irregularity in multi-dimensional space-filling curves with applications in multimedia databases,” in *Proceedings of the 2001 ACM CIKM*. ACM, 2001, pp. 512–519.
- [53] —, “On query processing and optimality using spectral locality-preserving mappings,” in *International Symposium on Spatial and Temporal Databases*. Springer, 2003, pp. 102–121.
- [54] R. S. Sutton and A. G. Barto, *Reinforcement learning - an introduction*, ser. Adaptive computation and machine learning, 1998.
- [55] E. Liang, H. Zhu, X. Jin, and I. Stoica, “Neural packet classification,” in *Proceedings of the ACM Special Interest Group on Data Communication*, 2019, pp. 256–269.